XXI IMEKO World Congress "Measurement in Research and Industry"
August 30 – September 4, 2015, Prague, Czech Republic

SOME ASPECTS OF MOLECULAR PHYSICS IN MEASURING TISSUE SAMPLES USING ENOSE FOR DISEASE DIAGNOSTICS

Markus Karjalainen [1], Antti Roine [2] Niku Oksala[3], Jukka Lekkala[1]

[1] Department of Automation Science & Engineering, Tampere University of Technology, Tampere, Finland, markus.karjalainen@tut.fi, jukka.lekkala@tut.fi
[2]Medical School, University of Tampere, Tampere, Finland, antti.n.roine@gmail.com
[3] Department of Surgery, Medical School, University of Tampere & Department of Vascular Surgery, Tampere University Hospital, Tampere, Finland, niku.oksala@uta.fi

Abstract – eNose technologies can be used for disease diagnostics. One technology is based on ionized molecules and their drifting speed in an electric field. Ionized molecules can be measured with ion mobility spectrometry and with electrical mobility measurements. Depending on the size scale of these molecules, different physical effects are relevant. We studied the relevance of size scale dependent physics for disease diagnostics.

Keywords: aerosol physics, ion mobility spectrometry, disease diagnostics

1. INTRODUCTION

Cancer is a leading cause of death in developed countries and second leading cause in undeveloped countries [1]. Early cancer diagnosis can reduce mortality significantly. Olfactory detection of cancer is an emerging diagnostic method [2], [3]. In most solid cancers, surgical resection of malignant tissue with healthy margins remains the definitive curative treatment. Discriminating malignant from healthy tissue by microscopy is laborious and slow. Rapid detection by smelling is proposed to improve the surgical procedure [4]. Diagnosing other diseases with artificial olfactory systems such as infections have recently been reported [5].

Smelling is based on identifying molecules by their chemical attributes. Molecule conditions are affected by several physical and chemical effects. By manipulating these effects, the properties of molecules can be measured. Molecules should be volatile, detectable, and carry information about the detectable tissue. Information from the tissue can be gained by the analysis of the composition of these molecules. Depending on sampling methods some unwanted substances are introduced to the sample, simultaneously with the indicator substance. Water from the sample can mask signals from other molecules and decrease the information available on the sample. Large molecule clusters cannot be identified with olfactory technologies and they will usually contaminate specific sensing systems by introducing large amount of substance into the sensor.

Generally larger molecules carry more information about the original function of the tissue. They tend to serve for more specific purposes than smaller molecules, which are distributed more uniformly in the tissue. Metabolomics studies chemical fingerprints that specific cellular processes leave behind [6]. Metabolome refers to the complete set of small molecule chemicals found in a biological sample [7]. These molecules are generally less than 1.5 kilodaltons of weight. The heaviest of these are non-volatile in normal temperature and pressure conditions NTP. Odours from unbalanced metabolic situations can be used in disease diagnostics [8]. Larger biological molecules consist of proteins, peptides and DNA which are studied in proteomics and in genomics. These have an advantage of containing more detailed information about the source, but require complicated study methods. Small metabolic molecules are naturally vaporized in NTP conditions and so easily delivered to artificial olfactory sampling system. Larger molecules need some preconditioning.

Compound volatility is a loose function of molecular size. Molecule polarizability increases when the space where electrons can move freely increases. In small molecules, electrons are more bound than in large ones [9]. Loose electrons in nonpolar molecules interact with polar molecules. These interaction forces are called Debye forces. Molecules are also induced mutually temporal dipoles which draw these molecules, the force called as London force, a particular case of van der Waals force. Van der Waals forces are dependent on Hamaker constant which is defined for molecule pairs on a specific medium [10]. J. F. Pankow and W. E. Asher have developed more sophisticated models for predicting organic compound volatilities for different molecules [11]. As compound volatility and partial pressure in gas phase decreases boiling point increases. A volatile organic compound (VOC) has definition in European Union directive as a compound having boiling point less or equal to 250 °C in NTP-conditions [12]. For this boiling point, molecular weight can vary from tens of daltons up to several hundreds of daltons depending on the compound structure. Molecules with strong polarity like water have a high boiling point compared with its size. Long molecules have more freedom for electrons than short ones having a higher boiling point. The high boiling point and so a low vapor pressure, cause molecules to be less abundant in gaseous form and so more challenging to detect. These substances do

not evaporate in normal conditions. Proteins and peptides can be artificially evaporated with methods like thermal desorption, electrospray ionization (ESI), laser ablation, or directly bombarding the sampling surface with ions [13]. Molecules vaporized above their partial pressure tend to form clusters when colliding with each other. These clusters are studied in aerosol physics.

2. METHODS

2.1 Measurement methods

For a gas phase and particle phase there are several different measurement methods. Here we focus only on methods which use ionized molecules in NTP conditions. In Ion Mobility Spectrometry (IMS) and in Electrical Mobility Measurement, these ionized molecules are separated according to their drifting speed in a carrier gas, which is often air. Drifting velocity is defined as particle's electrical mobility (1) [14]. This equation is used in aerosol measurements for particles from 100 nm down to 1 nm of characteristic length. For larger particles, turbulence has to be taken into account.

$$Z = \frac{V_{te}}{E} = \frac{neC_c}{3\pi\eta d} \; for \; Re < 1, \qquad (1)$$

where $V_{te}$is the particle velocity, e is electric charge, and n is the amount of particles. C_c is a slip correction factor, η is viscosity, Re is Reynolds number, and d is the particle diameter. For the IMS, the drifting principle is the same, but the size scale is smaller, from 0.1 nm to a few nanometres. For small molecules, the drifting velocity can be estimated with the 12,4 hard-core potential model presented by L. A. Viehland [15], [16], where the molecule mobility is estimated to follow a corrected molecule radius to power 12, minus corrected molecule radius to power 4. This estimates the nuclear attractive and repulsive forces, but not exactly the van der Waals forces which attract to the power of minus 6 as a function of the distance.

Ion mobility measurements have a few different configurations but a generic device principle is presented in Fig. 1. Numerous different ionization sources can be used and drifting region principles vary depending on the measurement method. In a time of flight ion mobility spectrometer (TOFIMS) ions drift a certain length in a constant electric field and the drifting time is measured. In travelling wave IMS ions are pushed with moving electric field waves. In this method, the molecules drifting speed are in the power of two, when compared with the molecules cross sectional area, with a TOFIMS that is linearly dependent. Third type is an aspiration IMS (aIMS) where ions are moving in a drift gas flow and the electric field is perpendicular to the gas stream, as seen in Fig. 2. A closely related configuration is a differential mobility analyser (DMA). DMA and aIMS have the main difference in variable electric field and constant detection spot, in the aIMS it is opposite.

Fig. 1. A generic ion mobility measurement setup: First sample is introduced to the device. Secondly the sample is ionized in a reaction region. In third step ions drift in the mobility region and are eventually detected in the detector.

The drifting speed is dependent on the aerodynamic diameter and number of electric charges of ions. In a differential mobility analyser (DMA), which is used in aerosol measurements, ions drift between parallel tube walls and ions with desired mobility are captured to a separate flow channel. With the aIMS ions collide with electrodes and lose their charge in a single flow channel.

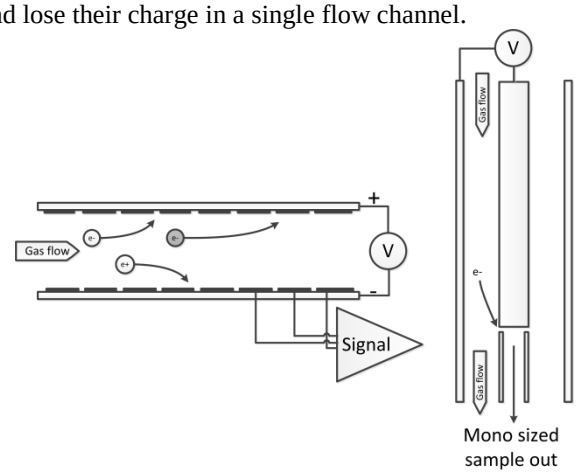

Fig. 2. aIMS (left) and DMA (right) configurations. In aIMS charged ions move through a perpendicular electric field with a gas flow and drift towards the electrode plates according to their electrical mobility. The electric charge is measured when ions hit to electrodes. In DMA ions move through the perpendicular electric field and ions with right mobility drift through a gap to a separate flow channel.

2.2. Atmospheric particle formation and evaporation

If molecules are forcefully driven from a liquid sample to gaseous form, as in ESI, they can be vaporized if the partial pressure of the sample solution is above the partial pressure of carrier gas of the measurement instrument. Liquid particles under 100 nm of size can undergo vaporization above their normal partial pressure due to Kelvin effect. Charged liquid particles may be split into smaller particles if charge density exceeds Rayleigh limit [14]. In conditions ,where particles are vaporized above their partial pressure there is a tendency for molecules to form larger particles through condensation and coagulation. For solid air particles, thermal coagulation is called agglomeration. It is caused through a Brownian motion where free floating particles collide and are attached through van der Waals forces. Coagulation speed can be estimated through (2).

$$\frac{dN}{dt} = -4\pi d_p D N^2, \qquad (2)$$

where $\frac{dN}{dt}$ is the number concentration, d_p is particle diameter, and D is a diffusion coefficient [9]. Equation implies that the change in the particles number concentration is on a square, from the current number. Simultaneously an increase of volume in new particles is linear to the amount of the coagulated particles, as the volume increases on a cube root to a diameter; as is presented in (3).

$$d(t) = d_0(1 + N_0 4\pi d_p D t)^{1/3} \qquad (3)$$

Condensation of liquid particles is a reversible process unlike coagulation of solid particles. Condensation and evaporation are dependent on the partial pressure. Initially, condensation begins from a solid particle if it is present. Without the nucleus partial pressure has to be exceeded multiple times to ignite the condensation process. In Fig. 4 particle modes are representing particles, formed from a gas and vapour samples through molecule-to-particle conversion. In accumulation mode particles are coagulated from nucleated particles. Coarse particles are coagulated from accumulated particles and are affected with gravitation.

Coagulation speed is linearly dependent on absolute temperature. A spatial temperature gradient drifts particles towards a cold end of the gradient. This is known as a thermophoresis. Thermophoresis can be used as a principle for particle filtration and sampling.

2.3 Aerosol and molecule filtering

Aerosol particles are defined so that they are bound to walls when touched. This adhesion by collision is the most often used filtering method. Aerosol particles down to 100 nm tend to collide with walls or filter fibres with their inertia. Particles under 100 nm of diameter tend to collide with a diffusion movement. Particles around 100 nm are thus more challenging to filter out. [14] This may be beneficial for a virus spreading (Fig. 4) and illustrated in Fig. 3.

Aerosol particles can be filtered effectively with a diffusion and collision down to 0.5 nm [17] or 1.4 nm [18]. Adhesion study on this size scale is challenging due measurement instrument limitations. Smaller particles than these tend to bounce away from surfaces due to their inertial energy which is exceeding the adhesion energy. A smaller aerosol particle than approximately 0.5-1 nm, can be seen as a gas molecule. According to G. Moureta, S. Chazeleta, D. Thomas, and D. Bemer [17] adhesion efficiency of the particle is one, down to 0.5 nm particles, as in Fig. 3. The increase of diffusion movement speed on smaller size will improve particle filtration efficiency down to 0.5-1 nm particles. Due weaker adhesion efficiency smaller particles than these will not be bound on surfaces. The size limit for surface bounding is dependent on the Hamaker constant.

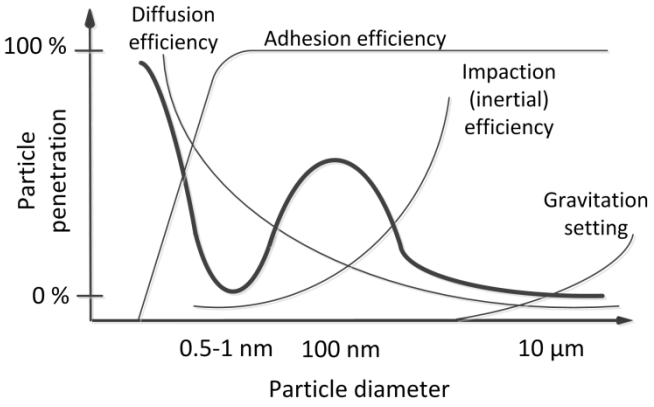

Fig. 3. A sketch from particle penetration as a function of the particle diameter. Particles smaller than 0.5-1 nm do not adhere on walls or filters fibers and so stay in gaseous form. Particles around 1 nm have a high collection rate through large diffusion. Particles around 100 nm are at a point where diffusion efficiency and inertial impaction do not efficiently collect particles. Particles bigger than 10 µm are affected by gravitation. [14],[17]

2.3. Molecule charging

Many, but not all artificial olfactory measurement methods have to charge the detectable molecules with an electric charge. These include mass spectrometry (MS) and IMS. Charging is done with diffuse charging methods: radioactive, photonic, corona discharge, electrospray, heat, flame, or plasma ion sources [13]. For macromolecules or particles larger than the order of 100 nm field charging is added for charging methods. Unfortunately, there is no practical method for detecting how many charges a single molecule has adsorbed. That is why there is no absolute method to determinate whether there is a large molecule

with several charges or a cluster of small molecules with a single charge. The probability for single charging decreases when the size of molecule increases. With diffusive charging mechanism, the charge probability follows a semi-empirical formula [14]. Typical results for charging probability is presented in Fig. 4 where ionizing gas concentration is 10^{13} ions·s/m^3. Electric field charging is dominant with particles larger than 200 nm. In Fig. 4, the calculated charging field was 500 kV/m. The measurement sensitivity is as well a function of molecules proton or electron affinity. Molecules with large affinity capture ions with higher probability. This is proportional to the gas phase acidity of the compound.

3. CONCLUSIONS

We measured urinary pathogens from urine with IMS [5]. These molecules are volatile organic compounds (VOC), what vaporize to sample headspace according to their partial pressure function. This vaporized gas has non-beneficial volatiles such as water, and biomarkers such as amines. From the perspective of total metabolic compounds in urine, only some parts would be vaporized. Large components such as lipids [19] are not vaporized. In case larger particles need to be vaporized, methods like ESI would be needed. DMA, ELPI and other aerosol measurement methods are not applicable as a component in metabolic compound research due to their inadequate molecule size measurement range.) Some applications could be found if a high concentration and large molecule sized sample are modified. Another application could be found on handling massive molecules as proteins, antibodies and large biological components as cells and viruses.

Genuine tissue samples have parts ranging on several different size scales, from water molecules to human cells. If all these need to be vaporized, several different physical effects should be taken into account depending on a particular size scale of the sample particle.

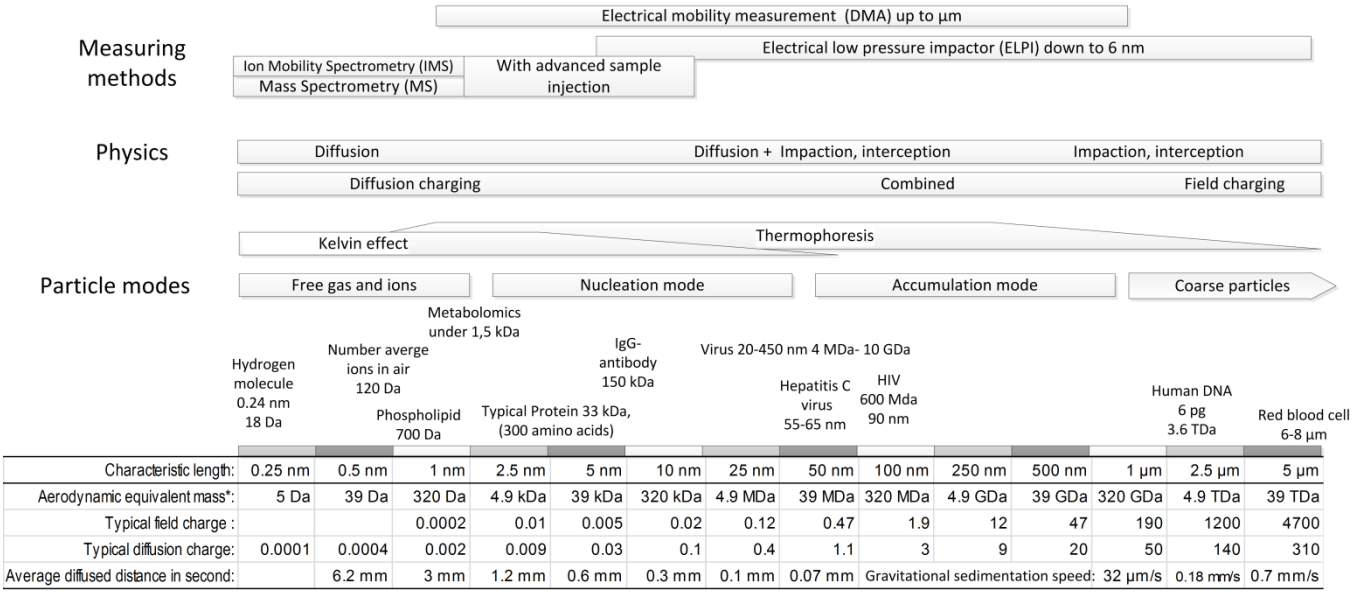

Characteristic length:	0.25 nm	0.5 nm	1 nm	2.5 nm	5 nm	10 nm	25 nm	50 nm	100 nm	250 nm	500 nm	1 µm	2.5 µm	5 µm
Aerodynamic equivalent mass*:	5 Da	39 Da	320 Da	4.9 kDa	39 kDa	320 kDa	4.9 MDa	39 MDa	320 MDa	4.9 GDa	39 GDa	320 GDa	4.9 TDa	39 TDa
Typical field charge :			0.0002	0.01	0.005	0.02	0.12	0.47	1.9	12	47	190	1200	4700
Typical diffusion charge:	0.0001	0.0004	0.002	0.009	0.03	0.1	0.4	1.1	3	9	20	50	140	310
Average diffused distance in second:		6.2 mm	3 mm	1.2 mm	0.6 mm	0.3 mm	0.1 mm	0.07 mm	Gravitational sedimentation speed:			32 µm/s	0.18 mm/s	0.7 mm/s

Fig. 4. Particle size distribution from small molecules to macromolecules, that are moderately affected by gravitation. The figure presents size scales where physics and measurement methods are valid. *Aerodynamic equivalent mass is a mass of a sphere diameter of characteristic length and 1g/cm^2 density. Typical field charge is an estimate for how many charges molecules receive on average. [13], [14]

REFERENCES

[1] A. Jemal, F. Bray, M.M. Center, J. Ferlay, E. Ward, & D. Forman, "Global cancer statistics" *CA Cancer Journal for Clinicians* vol. 61 pp. 69-90. Feb. 2011,

[2] A. Roine, M. Tolvanen, M. Sipiläinen, P. Kumpulainen, M.A. Helenius, "Detection of smell print differences between nonmalignant and malignant prostate cells with an electronic nose*." Future Oncol* 8: 1157–116, 2012

[3] A. Roine, E. Veskimäe, A. Tuokko, P. Kumpulainen, J. Koskimäki, et al. (2014) "Detection of prostate cancer by an electronic nose: a proof-of-principle study." *J Urol.* doi: 10.1016/j.juro.2014.01.1

[4] J. Balog, T. Szaniszlo, K.-C. Schaefer, J. Denes, A. Lopata, L. Godorhazy, D. Szalay, L. Balogh, L. Sasi-Szabo, M. Toth, Z. Takats, "Identification of Biological Tissues by Rapid Evaporative Ionization Mass Spectrometry*", Anal. Chem.* (2010), 82, 7343–7350

[5] A. Roine, T. Saviauk, P Kumpulainen, M. Karjalainen, A. Tuokko, J. Aittoniemi, R. Vuento, J. Lekkala, T. Lehtimäki, T. L. Tammela, N. K.J. Oksala, "Rapid and accurate detection of urinary pathogens by mobile ion mobility

spectrometry -based electronic nose: a proof-of-principle study", *Plos one*, 20 December 2014.

[6] D. Bennett "Growing pains for metabolomics". *The Scientist* vol. 19 (8), pp. 25–28, April 2005.

[7] S. G. Oliver, M. K. Winson, D. B. Kell, F. Baganz, "Systematic functional analysis of the yeast genome". *Trends Biotechnol.* vol. 16 (9) pp. 373–378, September 1998.

[8] G. A. N. Gowda, S. Zhang, H. Gu, V. Asiago, N. Shanaiah, D. Raftery. "Metabolomics-Based Methods for Early Disease Diagnostics: A Review", *Expert Rev Mol Diagn.* vol. 8 (5) pp. 617–633 September 2008.

[9] E. V. Anslyn, D. A. Dougherty *Modern Physical Organic Chemistry*. University Science, 2006.

[10] F. L. Leite, C. C. Bueno, A. L. Da Róz, E. C. Ziemath, O. N. Oliveira Jr. "Theoretical Models for Surface Forces and Adhesion and Their Measurement Using Atomic Force Microscopy", *Int. J. Mol. Sci*., vol. 13 (10), 12773-12856, October 2012.

[11] J. F. Pankow, W. E. Asher, "SIMPOL.1: a simple group contribution method for predicting vapor pressures and enthalpies of vaporization of multifunctional organic compounds". *Atmos. Chem. Phys*., 8, 2773-2796, May 2008.

[12] Directive 2004/42/CE of the European Parliament and of the Council of 21 April 2004 on the limitation of emissions of volatile organic compounds due to the use of organic solvents in certain paints and varnishes and vehicle refinishing products *EUR-Lex*, European Union Publications Office. Retrieved on 2010-09-28.

[13] G.A. Eiceman, Z. Karpas, H.H. Hill, Jr. *Ion mobility Spectrometry*, CRC Press, Boca Raton, 2014

[14] W. C. Hinds, *Aerosol Technology, properties, behaviour, and Measurement of Airborne Particles*, A Wiley-intercience, New York 1999

[15] P. V. Johnson, H. I. Kim, L. W. Beegle, I. J. Kanik, "Electrospray Ionization Ion Mobility Spectrometry of Amino Acids: Ion Mobilities and a Mass-Mobility Correlation" *J. Phys. Chem. A*,vol. 108, 5785-5792, May 2004.

[16] L. A. Viehland, E. A. Mason, Gaseous ion mobility and diffusion in electric fields of arbitrary strength, *Ann Phys. N. Y,*. vol, 110, pp. 287–328 February 1978.

[17] G. Mouret, S. Chazelet, D. Thomas, D. Bemer, "Discussion about the thermal rebound of nanoparticles," *Separation and Purification Technology*, vol. 78, pp. 125–131, April 2011

[18] C. S. Kim, L. Bao, K. Okuyama, M. Shimada, H. Niinuma "Filtration efficiency of a fibrous filter for nanoparticles", *Journal of Nanoparticle Research* vol. 8, pp. 215–221, July 2006.

[19] S. Bouatra, F. Aziat, R. Mandal, A. C. Guo, M. R. Wilson, C. Knox, T. C. Bjorndahl, R. Krishnamurthy, F. Saleem, P. Liu, Z. T. Dame, J. Poelzer, J. Huynh, F. S. Yallou, N. Psychogios, E. Dong, R. Bogumil, C. Roehring, D. S. Wishart, "The Human Urine Metabolome*", PLOS one*, 4 September, 2013.